Effects of Measurement Materials and Oxygen Partial Pressure on the Viscosity of Synthetic Eastern and Western United States Coal Slags

ARTICLE *in* ENERGY & FUELS · JUNE 2013

Impact Factor: 2.79 · DOI: 10.1021/ef300632x

energy&fuels

Article

pubs.acs.org/EF

Effects of Measurement Materials and Oxygen Partial Pressure on the Viscosity of Synthetic Eastern and Western United States Coal Slags

Jingxi Zhu,*[,†,‡] Tetsuya Kenneth Kaneko,[†,‡] Haoyuan Mu,[‡] James P. Bennett,[§] and Seetharaman Sridhar[†,‡]

[†]National Energy Technology Laboratory, United States Department of Energy, Pittsburgh, Pennsylvania 15236, United States
[‡]Department of Materials Science and Engineering, Carnegie Mellon University, Pittsburgh, Pennsylvania 15213, United States
[§]U.S. Department of Energy, National Energy Technology Laboratory, Albany, Oregon 97321, United States

ABSTRACT: The viscosity of the molten ash (slag) resulting from the mineral constituents in carbon feedstock used in slagging gasifiers is critical for controlling the gasification process. The viscosity of two synthetic slags with compositions resembling the mineral impurities in average eastern and western coal feedstock was examined at temperatures from 1300−1500 °C using a rotating bob viscometer. A few combinations of atmospheres and experimental materials were investigated with respect to one another to determine slag viscosity. A CO/CO_2 atmosphere (CO/CO_2 = 1.8, corresponding to a $P_{O_2} = 10^{-8}$ atm) is required to sustain ferrous ions in FeO-containing slags, an environment that is oxidizing to most metals. Iron oxide in the slag prevents usage of Fe parts. In unpurified Ar, the Fe metal surface oxidizes. Using purified argon prevents iron measurement components from oxidation; however, the metallic surfaces act as nucleation sites for the reduction of the Fe oxide in the slag into metallic Fe. Dissolution of ceramic materials into the slag, including Al_2O_3 and ZrO_2, occurs in both atmospheres. Therefore, evaluating slag properties in the laboratory is challenging. The measured viscosities of two synthetic slags in this study diverged depending upon material selection. This difference is likely attributable to container/spindle-slag interactions. Viscosity measurements of the eastern coal slag using all ceramic parts agreed best with FactSage prediction above 1350 °C, with an average activation energy of 271.2 kJ. For western coal slag, the dissolution of container/spindle materials was substantial during the measurement, with precipitation of crystalline phase noted. The experimental viscosity data of the western coal slag agreed best with Kalmanovitch prediction above 1350 °C. The activation energy changed dramatically for both data sets of western coal slag, likely indicating the Newtonian-to-non-Newtonian transition.

1. INTRODUCTION

Gasification allows for the generation of clean power from lower cost solid fuels, such as western coal and petcoke. Among various technologies, high-temperature slagging gasifiers have the potential to co-gasify fuels, such as petroleum byproducts and biomass waste, which would increase fuel flexibility, lower the net CO_2 output and emissions, and be adaptable to carbon capture and storage (CCS) to achieve near-zero air emissions. In integrated gasification combined cycle (IGCC) power systems, the pollutants are converted into reusable byproducts and the excess heat is used in a steam turbine. However, issues related to the maintenance and reliability of the gasifer need to be addressed. The difficulties are largely related to the inorganic constituents in the fuel feedstock. In a slagging/entrained flow gasification system, the inorganic constituents leave the gasifier as a molten slag. Carbon feedstock materials, which can include coal, petroleum coke (petcoke), biomass, or mixtures of these materials, contain numerous minerals that liquefy under the gasification conditions [T = 1325−1600 °C; P = 2.07−6.89 MPa; and $\log(P_{O_2})$ = from −9 to −7].[1] The liquefied ash coalesces and forms a slag. The composition, structure, and resulting properties of the slag are critical to the operation of the gasifier. Dependent upon the slag properties, it can either be too viscous and clog slag flow from the gasifier or be too fluid and cause excessive degradation of the refractory liner.[2] Improvements in both of these areas can enhance the commercial competitiveness of IGCC technology, which, in turn, can lead to improved economics of its use with CCS.

Slag viscosity and precipitation kinetics are impacted by the degree of polymerization and the size and shape of the polymeric units. Both of these structural features will vary as the slag drains downward along the sidewall or infiltrates into the refractory. They will also vary according to the partial pressure of oxygen, which is determined by the CO/CO_2 ratio in the gasifier. Ash composition depends upon the source of the coal and/or any additional carbonaceous feedstock, such as petcoke. For example, western U.S. coal in comparison to eastern U.S. coal is significantly richer in CaO,[4] which is a strong depolymerizing unit. Eastern coal, on the other hand, contains significant amounts of Fe oxides, but their depolymerizing ability depends upon the oxidation state of Fe, which is influenced by the oxygen partial pressure in the gasifier. Evaluations of molten coal ash viscosity are abundant for binary (such as $CaO-SiO_2$, $FeO-SiO_2$, and $Al_2O_3-SiO_2$), ternary (such as $CaO-FeO-SiO_2$, $Al_2O_3-FeO-SiO_2$, and $Al_2O_3-CaO-SiO_2$), quaternary (such as $Al_2O_3-CaO-FeO-SiO_2$), and high-order systems.[5] A lot of these studies have been conducted under inert atmospheres using rotating bob viscometry with either metallic (Mo or Fe) or

Received: April 13, 2012
Revised: June 12, 2012
Published: June 13, 2012

   dx.doi.org/10.1021/ef300632x | Energy Fuels 2012, 26, 4465−4474

Table 1. Source and Purity Levels (wt %) of the Oxide Components Used for Synthetic Slags

	mineralogical components				high-purity chemicals			
	IMSIL	wollastonite	olivine	G200	sodium carbonate	R2501	Al_2O_3	$CaCO_3$
sources	Unimin Specialty Minerals	NYCO Minerals	Bureau of Mines	The Feldspar Corporation	Alfa Aesar	Nubiola Group	AEE/Micron Metals	Aldrich Chemical Co.
Al_2O_3	0.752	0.34	0.16	18.28			99.90	
SiO_2	98.55	51.60	40.50	66.69			0.10	
Fe_2O_3	0.075	0.77	17.462	0.093		97.00		
CaO	0.032	46.15	0.204	0.57				99.00
MgO	0.037	0.38	50.677					
Na_2O	0.012		0.015	2.93	99.90			
K_2O	0.075	0.05	0.005	11.00				
TiO_2	0.042							

Table 2. Target and Premelted Composition of Synthetic Slags for Eastern Coal (EC) Slag and Western Coal (WC) Slag

wt %	Al_2O_3	CaO	Fe_2O_3	K_2O	MgO	MnO	Na_2O	P_2O_5	SiO_2	TiO_2	ZrO_2
EC-target	26.46	6.14	17.91	1.51	1.31		0.91		45.77		
EC-B1-VS	27.33	6.15	17.05	2.52	1.21	0.043	0.72	0.008	44.85	0.08	0.038
EC-B2-VS	26.02	6.54	18.42	2.24	1.28	0.042	0.75	0.022	44.47	0.085	0.035
WC-target	16.88	25.97	11.89	1.10	7.29		5.99		30.87		
WC-B1-VS	21.69	25.77	10.53	1.41	6.05	0.098	5.25	0.017	28.87	0.033	0.07

ceramic materials in contact with the slag. Several estimation models have been proposed, including the Urbain,[6] Browning,[2] FactSage,[7] and Kalmanovitch[8] models.

The aim of this work is to measure viscosities of synthetic slags with compositions corresponding to ash from two U.S. coal sources (western and eastern) under thermal and atmospheric conditions that are similar to those in a gasifier. Most significantly, this constraint entails carrying out viscosity measurements under a CO/CO_2 ratio of 1.8, which corresponds to an oxygen partial pressure of 10^{-8} atm. This selection in atmosphere poses a challenge with respect to the optimal selection of materials for the crucibles and spindles that are in contact with the melt. The atmosphere is oxidizing with respect to iron and molybdenum, while ceramic parts can dissolve into the slag. Therefore, a purified Ar atmosphere must be used for metallic parts. Platinum is problematic at high Fe oxide content, which has Fe dissolution into the Pt.[9] This viscosity study aims to address the following: (i) establishment of whether measurements carried out in inert atmospheres cause FeO conversion into Fe within the time of the measurement and whether this influences the measured viscosity, (ii) determination of whether excessive dissolution of ceramic parts (Al_2O_3 and ZrO_2) into the slag alters the slag chemistry and measured viscosity, and (iii) determination of whether the measured viscosities of synthetic slags with chemistries similar to U.S. coal ashes agree with available model predictions.

2. EXPERIMENTAL SECTION

2.1. Sample Preparation. Two synthetic slags with compositions resembling the mineral impurity constitution of United States coal feedstocks in entrained-flow slagging gasifiers were used in this investigation. First, a representative slag composition was selected by taking an average of ash constituents derived from sub-bituminous coal feedstock from the United States as reported by Selvig and Gibson,[3] which will be referred to as eastern coal (EC) from hereon. Second, a slag representing the ash composition of coal from the western United States (WC) was designed, averaging ash compositions of the Wyodak–Anderson and Beulah–Zap seams reported by Vorres.[4] The individual oxide components in powder form were mixed to their appropriate ratios. Both inexpensive mineralogical components and high-purity chemical components were used (details can be found in Table 1). The mixed powder was then melted and equilibrated in a gas mixture of CO/CO_2 with a ratio of 1.8, corresponding to an oxygen partial pressure of 10^{-8} atm. FactSage calculations indicated that, at the particular oxygen partial pressure, the Fe oxide should be 99.92 atomic % in the form of FeO and 0.08 atomic % in the form of Fe_2O_3. Upon extraction of the vitreous material from the crucible, the slag was ground to particles roughly 2 mm in size. For the synthetic eastern coal slag, dissolution of the Al_2O_3 crucible was minimal, with roughly a 1 wt % increase in the Al_2O_3 concentration observed. In contrast, Al_2O_3 crucible dissolution was more substantial with the synthetic western coal slag, with approximately a 5 wt % increase in the Al_2O_3 concentration noted. The target compositions and the slag compositions after melting are listed in Table 2. The slag compositions were evaluated using X-ray fluorescence (XRF) spectrometry. The letter "B" in the sample labels stands for "batch" and is followed by the batch number. The virgin slag of each batch is labeled "B*X*-VS"; eastern coal slags are labeled with "EC", and western coal slags are labeled with "WC".

Figure 1 shows the X-ray diffraction (XRD) spectra of the starting slags. The starting eastern coal slag was amorphous, while the starting western coal slag was partially crystalline. Western coal slag segregated into two parts after being remelted in a CO/CO_2 atmosphere: a crystalline part and a noncrystalline part. The major crystalline phases

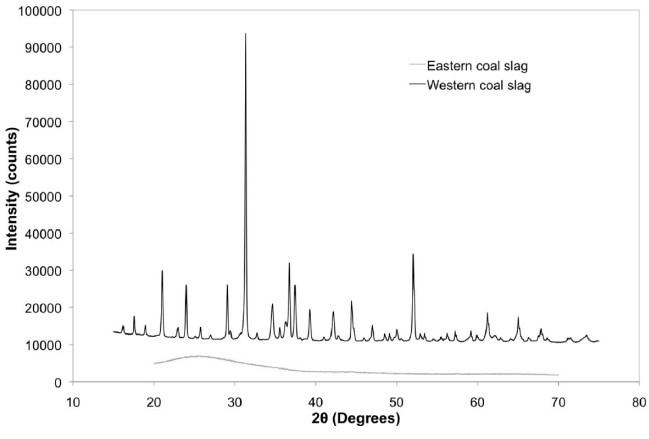

Figure 1. XRD of the starting slags of eastern and western coal slag.

dx.doi.org/10.1021/ef300632x | *Energy Fuels* 2012, 26, 4465–4474

Table 3. Materials and Atmospheres Used in This Study

measurement number	slag	spindle	crucible	atmosphere	P_{O_2} (atm)
EC-B1-M1	fresh	iron	ZrO_2	Ar (purified)	10^{-7}–10^{-8}
EC-B1-M2	recycled from measurement 1	iron	iron	Ar (purified)	10^{-7}–10^{-8}
EC-B1-M3	recycled from measurement 2	iron	iron (used in measurement 2)	Ar (purified)	10^{-7}–10^{-8}
EC-B2-M1	fresh	Al_2O_3	Al_2O_3	CO/CO_2	10^{-8}
EC-B2-M2	fresh	Al_2O_3	ZrO_2	CO/CO_2	10^{-8}
EC-B2-M3	fresh	Al_2O_3	Al_2O_3	UHP Ar (purified)	10^{-17}–10^{-18}
WC-B1-M1	fresh	Al_2O_3	Al_2O_3	CO/CO_2	10^{-8}
WC-B1-M2	fresh	Al_2O_3	ZrO_2	CO/CO_2	10^{-8}
WC-B1-M3	fresh	Al_2O_3	ZrO_2	CO/CO_2	10^{-8}

were determined by XRD to be $Ca_2Al_2SiO_7$ (gehlenite), $Ca_2MgSi_2O_7$ (akermanite), $FeAl_2O_4$ (hercynite), and $MgAl_2O_4$ (spinel). To mix the two parts well for the viscometry experiment, the western coal slag was crushed into a fine powder and ball-milled for 2 days.

A combination of spindle and crucible materials was used and is listed in Table 3. The iron spindles and crucibles were machined from 1018 steel (0.18% C). The gas atmospheres were either a pre-prepared mixture of CO/CO_2 with a ratio of 1.8 or Ar (ultra high purity) purified through a getter system of heated Mg turnings. All of the gases were supplied by Valley National Gas, Inc.

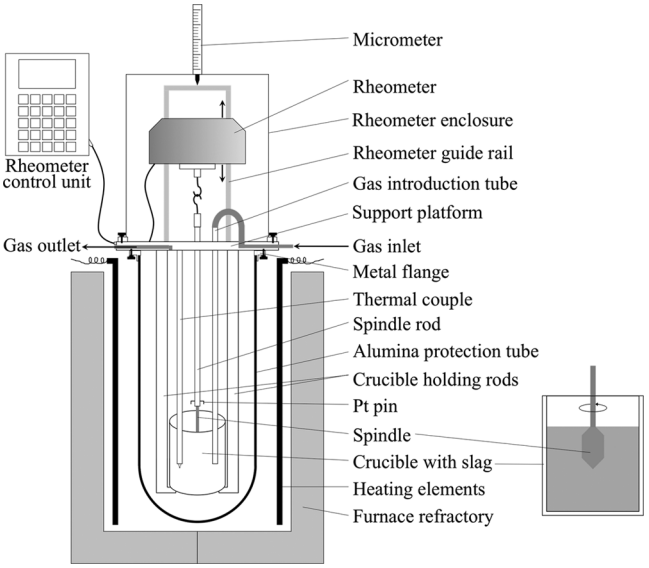

Figure 2. Schematic of the viscometer setup.

2.2. Measurements. *2.2.1. Viscosity Measurement.* The experimental setup is shown in Figure 2. The viscosity measurements were carried out using the rotating cylinder method. The core component of the viscometer is the Brookfield rheometer (model DV-III). The rheometer controls the rotation speed of the spindle, measures the torque exerted on the spindle, and converts the information into a viscosity reading. The full-scale torque of the viscometer is 7.187×10^{-4} N m. The rheometer can also be moved up and down along a guide rail, and the magnitude of such movement can be measured using a micrometer. The entire rheometer assembly is bolted onto a supporting platform inside an enclosure that is airtight.

The crucible filled with slag was steadily held by a set of three alumina rods and enclosed in an alumina protection tube attached to a metal flange. A thermocouple was placed in contact with the wall of the crucible, whose reading was used by an Eurotherm (model 818) temperature controller to control the output power to the heating elements. The reaction gas flows into the alumina protection tube through a gas introduction tube located next to the crucible and then escapes from the gas outlet built into the support platform. Iron and Al_2O_3 spindles of the same dimensions were used in the measurements. The viscometer was calibrated at 298 ± 0.1 K before each measurement using three oil standards with viscosities of 4.95, 12.16, and 58.56 Pa s.

In a general measurement, after placing the crucible with the premelted slag onto the beaker holding rods and mounting the spindle onto the spindle rod, the alumina protection tube was sealed by bolting the metal flange to the supporting platform. The spindle was suspended about 3 cm above the crucible top by raising or lowering the rheometer along the guide rail by a motorized drive. Before heating, the reaction chamber was flushed with reaction gas for 1 h. A continuous flow of the reaction gas was maintained at a flow rate of 0.2 ± 0.01 L/min during the entire course of the measurement.

The slag was heated to the designated temperature using the temperature profile pre-programmed into the temperature controller. The initial heating rate was 5 °C/min. Once the targeted temperature was reached, the slag was isothermally held to allow for stabilization. Next, the rotating spindle (typically at 5 rpm) was lowered toward the top of the liquid slag slowly until a sudden increase in the torque was read, which indicated the top of the melt was reached by the tip of the spindle. The spindle was then lowered 16 mm, and the slag/spindle system was maintained at the same temperature for 30 min to allow for the system to thermally stabilize.

When thermal equilibrium was obtained, viscosity measurements were carried out in a step-cooling cycle of 25 °C increments. For each temperature, the rotation rates were adjusted to achieve a roughly constant torque value between 70 and 80% of the full torque. Once the torque reading oscillated less than ±0.3%, the viscosity value was obtained by averaging within the oscillating range.

After the viscosity was measured at the lowest temperature, typically 1300 °C, the spindle was lifted to the starting position and the slag was rapidly cooled to room temperature. The slag composition was routinely analyzed by X-ray fluorescence (XRF) and XRD before and after each measurement. The slag/crucible and slag/spindle interfaced were also characterized with scanning electron microscopy (SEM).

2.2.2. Crystallization of Western Coal Slag. As noted in Figure 1, the western coal slag showed a tendency to crystallize, while the eastern coal slag did not. To assess the crystallization tendency of the western coal slag, a confocal scanning laser microscope (CSLM) was used for the study of the crystallization that had a gold image hot stage attached to the microscope. Details of the CSLM have been documented in the literature, but the key features of the system are (i) confocal optics with a source of the He–Ne laser (wavelength of 632.8 nm) allowing for imaging of features in a narrow focal plane while filtering background glare because of radiation and (ii) an infrared heating system, which allows for rapid heating and cooling. Using this system, crystal precipitation in semi-transparent slags or on the surface of opaque slags could be observed *in situ*.[10−13]

In each experiment, approximately 0.010–0.020 g of starting slag powder was poured into a cylindrical platinum crucible (99.99%, 5 $D \times 5$ $H \times 0.4$ T in mm), which was then placed into an Al_2O_3 crucible. The crucibles with slag were set on a platinum sampler pan and placed into the hot stage. Each starting slag powder in the Pt crucible was heated in the CSLM hot stage in a CO/CO_2 gas with a ratio of 1.8. The temperature profile shown in Figure 3 was used in each experiment. To

dx.doi.org/10.1021/ef300632x | Energy Fuels 2012, 26, 4465–4474

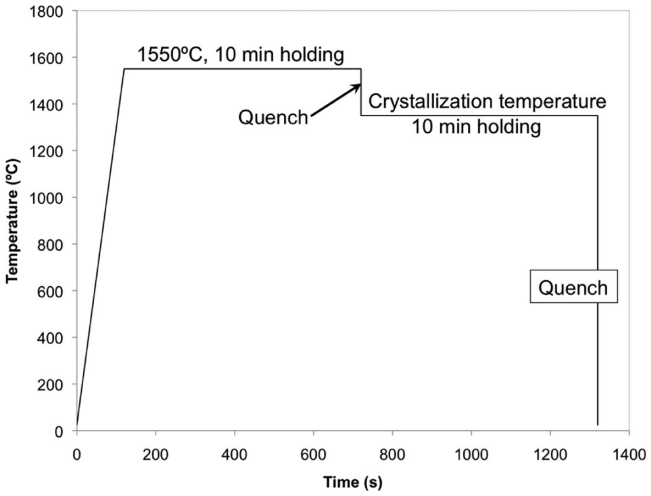

Figure 3. Temperature profile used for the crystallization study.

start from a completely molten slag, the slag powder was heated to 1550 °C and held for 10 min. The slag was then rapidly cooled (approximately 100 K/s) to the desired crystallization temperature, typically in a few seconds, and held isothermally for another 10 min. The slag crystallization event was optically observed and recorded *in situ*, and the time needed for the precipitation to occur on the surface of the slag liquid was recorded for each temperature. After crystallization had occurred at each crystallization temperature, the slags were quenched to room temperature to evaluate the crystallized phases using the SEM and XRD.

3. RESULTS

3.1. Eastern Coal Slag. Figure 4 shows the results of the viscometry experiments carried out for the eastern coal (EC)

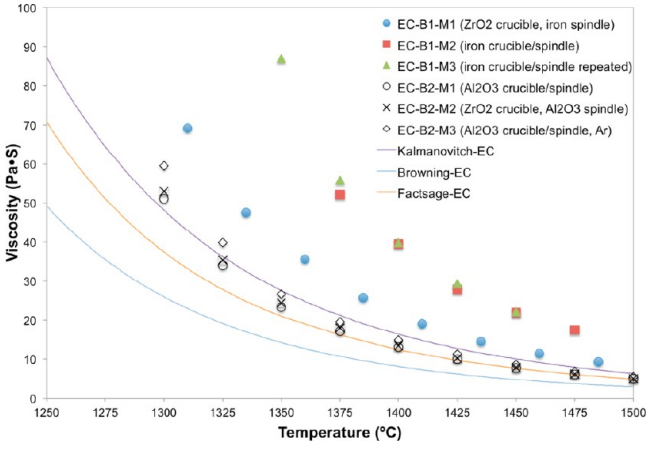

Figure 4. Measured and predicted viscosity versus temperature for the eastern coal slag.

slag, which is plotted along with model predictions according to refs 2, 7, and 8. The chemical compositions of the spent slags analyzed using XRF are listed in Table 4. Again, the letter "B" in the sample labels stands for "batch" and is followed by the batch number. The virgin slag of each batch is labeled "B*X*-VS", with "M" standing for post-measurement slag, followed by the measurement number. "EC" stands for eastern coal slags. Becuase the composition of the slag did not change significantly after the viscosity measurements, it was reasonable to calculate the model viscosity values using starting slag composition.

The following trends for viscosity can be noted: (i) The measurements carried out using an iron spindle and crucible in an inert Ar atmosphere consistently produced the highest viscosity values, while the measurements performed with all ceramic parts produced the lowest viscosity values. (ii) The measurement obtained using an iron spindle and a ZrO_2 container fell between the all ceramic and all iron systems. (iii) Measurements conducted using Al_2O_3 and ZrO_2 containers and Al_2O_3 spindle gauged similar/nearly identical viscosity values. For eastern coal slags, the pick-up of Al_2O_3 was small in all of the measurements using Al_2O_3 crucibles (no more than 0.7 wt %) and the pick-up of ZrO_2 from the crucible was even smaller (less than 0.35 wt %). (iv) The experiments carried out with all ceramic parts closely matched the predictions by FactSage and to a lesser extent with the model by Kolmanovitch. (v) When ceramic parts were used for viscosity measurements, the atmosphere was not found to have a noticeable effect on the viscosity.

Table 4 showed that the bulk slag compositions did not change appreciably after the viscosity measurements. When ceramic crucibles/spindles were used, the post-measurement slags picked up small amounts of Al_2O_3 or ZrO_2, which was the inevitable result of dissolution of crucible/spindle material into the slag during viscosity measurement. No large change in the Fe content in the spent slag was noted. Note that the chemical analysis could not indicate whether there was metallic Fe or ionic Fe in the slag. It was thought that the change in the bulk slag chemistry appeared to be small, regardless of the system. It should be noted, however, that FactSage indicated the slags were nearly saturated in Al_2O_3, which would account for the small Al_2O_3 container dissolution.[14] XRD scans of all of the post-measurement eastern coal slags were inconclusive on identifying the crystalline phase shown in Table 5, likely because the amount of crystalline material was too small in quantity. Therefore, the bulk slag, slag/crucible, and slag/spindle interfaces were further examined with SEM and energy-dispersive spectrometry (EDS).

Figure 5 shows the post-experiment characterization of slag/iron crucible interfaces. Significant amounts of metallic Fe were seen at the crucible interface. SEM examination of the bulk slag showed that the iron particles also became entrained within the slag. Furthermore, the slag/iron spindle interface had a very similar morphology. There were two possible sources that these iron particles could have come from: the FeO in the slag and the iron crucible. First, FeO in the slag could be reduced into metallic Fe because the oxygen potential was low enough to thermodynamically favor such a reaction. The oxygen partial pressure in purified Ar was determined by a ZrO_2 oxygen sensor to be on the order of 10^{-7}–10^{-8} atm. Kinetically, the decomposition of Fe oxide to Fe, in the absence of a reducing agent (such as carbon), would be expected to be very slow or even negligible. For this reason, it was surprising to find a minor amount of metallic Fe forming at the slag/crucible interface. On the other hand, the iron crucible wall may have assisted the precipitation of iron particles by providing nucleation sites.

Alternatively, a second possibility would be that metallic Fe could be entrained into the slag from the container walls. However, this was thought to be unlikely to have occurred, because a metallic surface would not spall, especially below the fusion temperature of Fe. This second mechanism would not be dependent upon the oxygen partial pressure.

In the case of the ceramic containers, the slag interacted with both Al_2O_3 and ZrO_2 crucible walls but in different manners. Figure 6a shows that needle-shaped crystals precipitate along the

dx.doi.org/10.1021/ef300632x | *Energy Fuels* 2012, 26, 4465–4474

Table 4. Chemical Analysis of Starting and Spent Slags for Eastern Coal Slag

wt %	EC-B1-VS	EC-B1-M1	EC-B1-M3	EC-B2-VS	EC-B2-M1	EC-B2-M2	EC-B2-M3
Al_2O_3	27.33	27.38	27.54	26.02	26.72	26.07	26.29
CaO	6.15	6.06	6.11	6.54	6.5	6.52	6.44
Fe_2O_3	17.05	16.61	16.17	18.42	18.31	18.28	18.18
K_2O	2.52	2.24	2.32	2.24	2.23	2.23	2.23
MgO	1.21	1.2	1.2	1.28	1.26	1.29	1.26
MnO	0.043	0.045	0.19	0.042	0.042	0.044	0.042
Na_2O	0.72	0.79	0.82	0.75	0.75	0.82	0.79
P_2O_5	0.008	0.031	0.02	0.022	0.023	0.027	0.024
SiO_2	44.85	45.14	45.35	44.47	44	44.35	44.55
TiO_2	0.08	0.06	0.066	0.085	0.067	0.067	0.069
ZrO_2	0.038	0.37	0.13	0.035	0.026	0.23	0.029

Table 5. XRD Analysis of the Post-measurement Slags

measurement number	XRD identified phases
EC-B1-M3	amorphous
EC-B2-M1	one peak, possibly of hercynite
EC-B2-M2	one peak, possibly of hercynite
EC-B2-M3	one peak, possibly of spinel

Al_2O_3 crucible wall. The EDS analysis indicated these crystals were most likely mullite ($3Al_2O_3{\cdot}2SiO_2$). XRD analysis on the slag showed the possible presence of hercynite. The crystal formation could also be a cooling effect.[15] On the other hand, the slag penetrated into the crucible wall, as seen in Figure 6b. The depth of such penetration averaged around 1−2 mm. EDS analysis revealed that there was no significant change in Al_2O_3 and FeO contents of the slag near the crucible wall.

Figure 7a shows the slag/ZrO_2 crucible interface. Figure 7b indicates that there is an increase in Zr content in the slag near the crucible sidewalls, but it is not dramatic. Indeed, the inductively coupled plasma (ICP) results in Table 4 did not show any appreciable change in the bulk slag composition.

Thus, as far as the slag/solid reactions on the crucible, both the Fe and ceramic systems resulted in unwanted phases, but when the data sets in Figure 4 were examined, the use of the Fe-based materials caused a larger deviation from predicted viscosity results. As mentioned earlier, an inert atmosphere is required for using Fe viscosity components, but as seen in Figure 5a, the reduction of FeO from the slag is significant. In the slags investigated, the oxidation state of Fe ions is the same in Ar or in the CO/CO_2 ratio found in gasifiers (ratio of 1.8). Therefore, on the basis of these interactions, it was decided that the ceramic systems would be the most suitable for the conditions of this study, and data sets EC-B2-M1, EC-B2-M2, and EC-B2-M3 were believed to be correct and agreed well with FactSage prediction until the temperature was below 1375 °C.

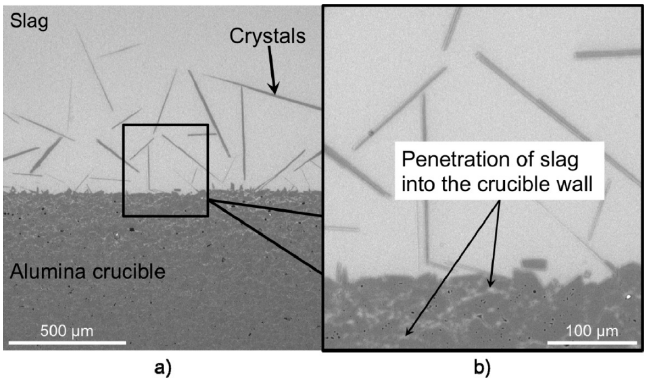

Figure 6. BSE micrograph of the (a) slag/Al_2O_3 crucible interface and (b) penetration of slag into the crucible wall.

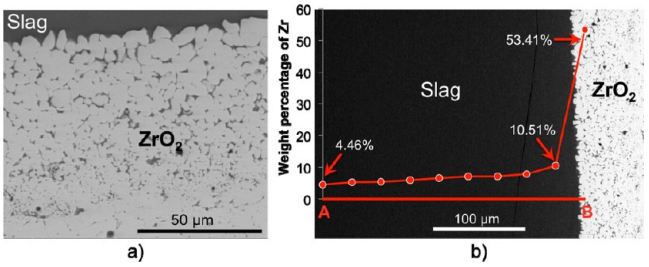

Figure 7. (a) SEM image of the slag/ZrO_2 crucible interface. (b) Zr composition profile along line AB.

Figure 8 shows the natural log of viscosities versus $1/T$ plot for eastern coal slags. The activation energies listed in this graph are based on the following equation:

$$\eta = A \exp\left(\frac{Q}{RT}\right) \quad (1)$$

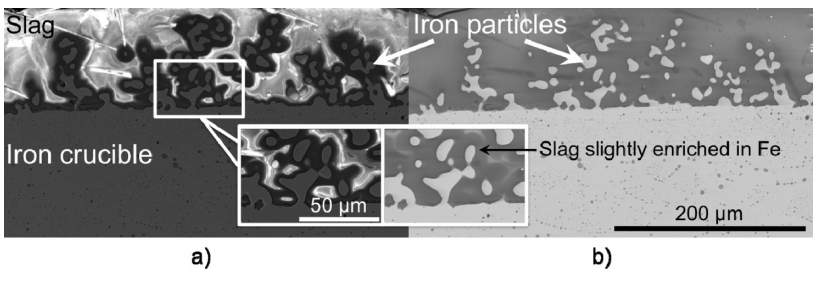

Figure 5. (a) Secondary electron (SE) and (b) backscattered electron (BSE) images of the slag/iron-crucible wall.

dx.doi.org/10.1021/ef300632x | *Energy Fuels* 2012, 26, 4465−4474

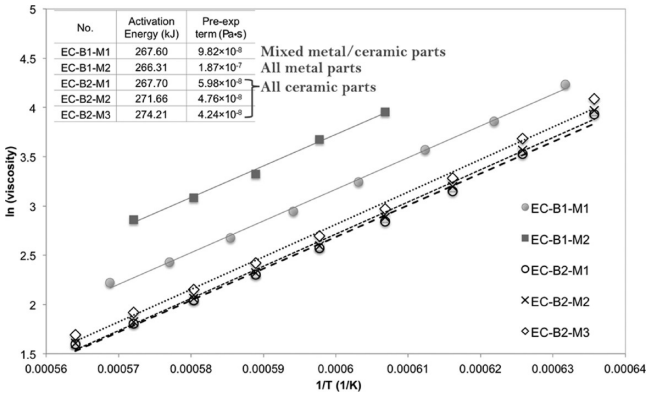

Figure 8. Natural log plot of viscosities for eastern coal slags.

where η is the viscosity in Pa s, Q is the activation energy in joules, and R is the gas constant.

The activation energies for the eastern coal slag data sets were similar, except for EC-B1-M3, which was not listed in Figure 8 to avoid confusion. The activation energy for EC-B1-M3 was about 17% higher than other data sets and could be attributed to the change in the slag chemistry because of recycling of the slag from the previous measurement, i.e., EC-B1-M2, during which some Fe^{2+} had left the slag and precipitated as metallic iron on the crucible wall.

3.2. Western Coal Slag. Western coal describes feedstock originating from the west of the Mississippi river. The western coal slag typically contains higher CaO and MgO contents than the slags from feedstock found further east. The increased concentrations of the alkali earth metal oxides cause the slag to have substantially different fusion temperatures, fluid properties, and chemical affinities toward refractory materials than its eastern coal slag counterpart. For this reason, the viscosity of western coal slag requires a comparison to that of the eastern coal slag.

Figure 9 plots the results of the viscosity measurements for the western coal (WC) slag. The predicted viscosity values were calculated using the same models as in the eastern coal slag study. However, because of the aggressive nature of the western coal slag, the slag compositions were found to have changed significantly after each viscosity measurement because of dissolution of the crucible/spindle material, as seen in Table 6. Again, the letter "B" in the sample labels stands for "batch" and is followed by the batch number. The virgin slag of each batch is labeled "B*X*-VS", with "M" standing for post-measurement slag, followed by the measurement number. Western coal slags are labeled "WC".

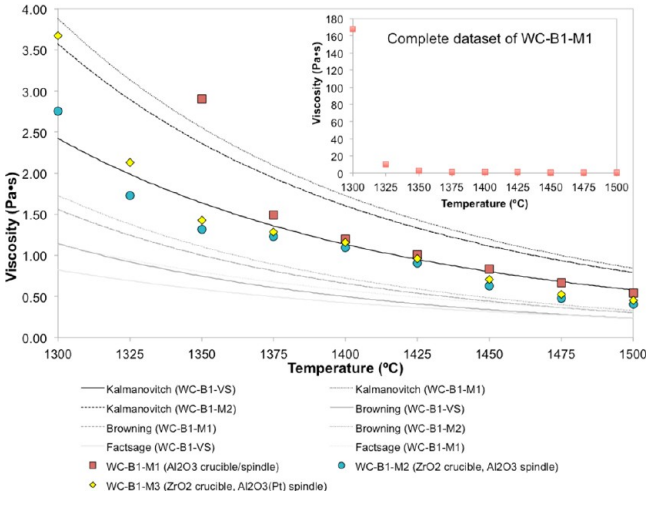

Figure 9. Measured and predicted viscosity versus temperature for the western coal (WC) slag.

Table 6. Chemical Analysis of Starting and Spent Slags for Western Coal Slag

wt %	WC-B1-VS	WC-B1-M1	WC-B1-M2	WC-B1-M3
Al_2O_3	21.69	31.12	23.21	22.87
CaO	25.77	22.5	20.9	23.24
Fe_2O_3	10.53	9.3	8.41	8.46
K_2O	1.41	1.19	1.13	1.22
MgO	6.05	5.42	5.28	5.5
MnO	0.098	0.086	0.086	0.096
Na_2O	5.25	4.58	4.2	4.76
P_2O_5	0.017	0.016	0.039	0.03
SiO_2	28.87	25.49	26.83	26.89
TiO_2	0.033	0.036	0.037	0.047
ZrO_2	0.07	0.004	9.64	6.66

Therefore, the model viscosity values were calculated using slag compositions of both before and after the measurements. The ZrO_2 content in the post-measurement slag was ignored for the following reasons: (i) None of the models considered in this paper took ZrO_2 into account. (ii) ZrO_2 has been reported to have little effect on the viscosity.[16]

It is noted in Figure 9 that the three measurements, in general, agreed best with the viscosity predictions of the Kolmanovitch model calculated with the starting slag composition.

The Kalmanovitch model fitted a large amount of experimental data, including those containing small fractions of crystalline solids, using the Weymann–Frenkel relationship. Therefore, the Kalmanovitch model predicts slag viscosities that contain fugitive solids mostly in the dilute range. On the other hand, the Browning model is not as adaptable in predicting viscosities for slags that are outside the Newtonian region, such as when a crystalline phase precipitates in a slag. The Browning model is based on the assumption that the viscosity–temperature curve is identical for all coal slags (in the Newtonian region), and thus, a standard curve is shifted along the temperature axis based on composition. Because of the semi-empirical nature of these models, the agreement with the experimental data changes within different composition ranges and with different experimental parameters. In the present study, it was believed that the disagreement between the experimental data and the prediction was mainly caused by a significant amount of crystal precipitated.

For measurement WC-B1-M1, the viscosity data set was characterized by an inflection point around 1350 °C, which was more evident in the natural plot shown in Figure 10. It was observed during the measurement that, for temperatures above 1375 °C, the molten slag was Newtonian (i.e., the relationship between the torque and rotation speed of the measuring head was linear), whereas the slag was non-Newtonian below 1350 °C. The viscosity measured with the ZrO_2 crucible, WC-B1-M2 and WC-B1-M3, showed very different characteristics. Instead of a single inflection point, there was consistently a bump in the temperature range of 1400–1350 °C, which corresponded to the plateau in the natural log plot in Figure 10. Upon examination of the post-experiment slags, it was believed that the different slag

dx.doi.org/10.1021/ef300632x | Energy Fuels 2012, 26, 4465–4474

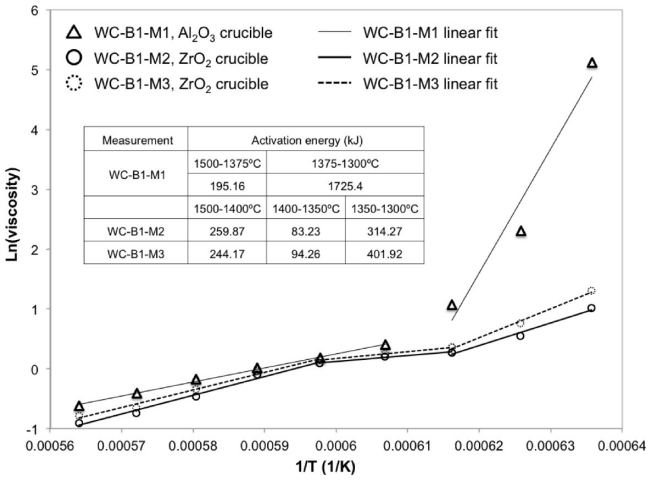

Measurement	Activation energy (kJ)		
WC-B1-M1	1500-1375°C	1375-1300°C	
	195.16	1725.4	
	1500-1400°C	1400-1350°C	1350-1300°C
WC-B1-M2	259.87	83.23	314.27
WC-B1-M3	244.17	94.26	401.92

Figure 10. Natural log plot for the two western coal slag viscosity measurements.

behavior in the measurements was largely caused by the different crystallization behavior of the slags contained in the different crucibles, i.e., Al_2O_3 and ZrO_2 crucible materials. Moreover, the viscosity of WC-B1-M3 in the 1300−1350 °C range was greater than WC-B1-M2 in the same temperature range, and this difference was believed to be caused by a greater extent of crystallization in the slag of the former because of a higher CaO content.

Figure 11 shows the crucibles after the two viscosity measurements. An Al_2O_3 crucible was used in WC-B1-M1, and a ZrO_2 crucible in WC-B1-M2. First, it was evident in panels a and b of Figure 11 that both crucibles were attacked by the slag, which resulted in significant dissolution of the crucible materials. Second, although the slags were quenched in the same manner in the two measurements, the crystallization of the slags was very different because the materials introduced into the slag played a different role in terms of crystallization.

The slag in the Al_2O_3 crucible was almost completely crystalline, as shown in Figure 11a. At the crucible/slag interface, dissolution resulted in an Al_2O_3 saturated slag layer was indicated by SEM−EDS evaluation at the region labeled S in Figure 11c. XRD identified the major crystalline phases in the bulk slag to be $Ca_2Al_2SiO_7$ (gehlenite), $Ca_2MgSi_2O_7$ (akermanite), $FeAl_2O_4$ (hercynite) and $MgAl_2O_4$ (spinel). Moreover, comparing the XRD patterns of the slag before and after the measurement, the relative intensity and positions of some peaks changed slightly. The peak shifts were associated with aluminum containing phases, i.e. gehlenite, hercynite and spinel. The introduction of Al_2O_3 from the crucible into the slag resulted in a significant change in the slag viscosity, and impacted the crystallization of the slag. The Al_2O_3 crucible wall may also act as a nucleation site that assists crystallization. With a significant amount of crystals

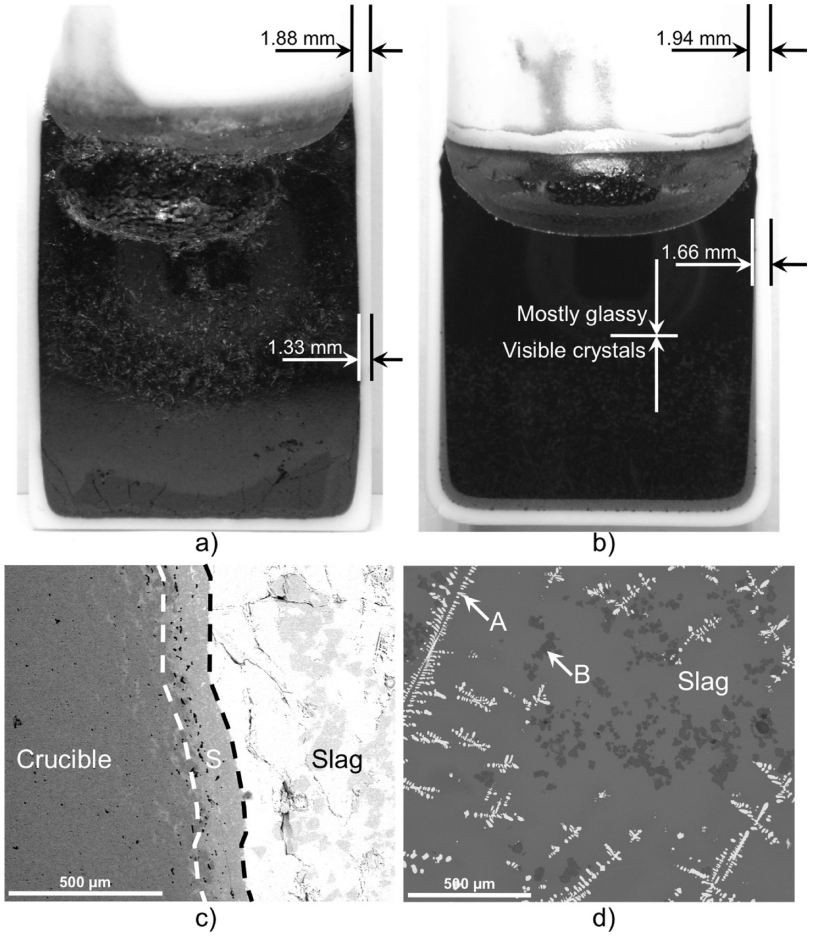

Figure 11. Optical images of cross-sectioned and polished crucibles after viscosity measurement for (a) WC-B1-M1 and (b) WC-B1-M2, and BSE micrographs of the post-measurement crucible and slag for (c) WC-B1-M1 (the region labeled with letter "S" is a layer saturated with Al_2O_3) and (d) WC-B1-M2 (crystals labeled with letter "A" and "B" are ZrO_2 and $MgAl_2O_4$, respectively).

dx.doi.org/10.1021/ef300632x | *Energy Fuels* 2012, 26, 4465−4474

precipitated, the slag changed from Newtonian to non-Newtonian at lower measuring temperatures.

The slag in the ZrO_2 crucible (WC-B1-M2) was partly glassy with some visible crystals. As shown in Figure 11d, unlike the slag in the Al_2O_3 crucible, the slag in the ZrO_2 crucible had only two crystalline phases, ZrO_2 and $MgAl_2O_4$, as determined by SEM–EDS and XRD analyses. The two crystalline phases are indicated in Figure 11d by "A" and "B", respectively. Because of the dendritic morphology of the ZrO_2 crystals, it was believed that ZrO_2 dissolved into the slag at high temperatures and reprecipitated when measuring viscosity at lower temperatures or upon cooling. There was also a ZrO_2 layer along the inner wall of the crucible. On the basis of the morphology of the ZrO_2 crystals in this layer, it was believed that this part of ZrO_2 crystals did not go into the liquid during measurement. The difference of ZrO_2 contents in the spent slag of WC-B1-M2 and WC-B1-M3 in Table 6 reflects the amount of ZrO_2 crystals in the layer along the inner crucible wall, because this ZrO_2 layer was removed from the spent WC-B1-M3 slag before XRF analysis, while this ZrO_2 layer was preserved in the spent WC-B1-M2 slag. The portion of the dissolved ZrO_2 (dendrites) that might have a bigger impact on the viscosity was about 6–7 wt %.

Despite dissolution and reprecipitation, ZrO_2 should have little impact on the viscosity, particularly at higher temperatures, if it is in liquid form,[16] but once ZrO_2 precipitates as solid, it should increase viscosity. The precipitation of $MgAl_2O_4$ crystals fits thermodynamic predictions made with FactSage, as shown in Figure 12. It was also noted that the Al_2O_3 spindle in the WC-B1-M2 and WC-B1-M3 was attacked much more severely than the spindle used in WC-B1-M1. The diameter of the spindle shrank more than 1.5 mm. On a rough estimation, this would result in an approximately 16.9% decrease in the surface area of the spindle measuring head that was in contact with the slag at the end of the measurement, and this would affect the torque measured. However, because the spindle was exposed to a gradually decreasing isotherm temperature history, there was no good way to measure or extrapolate the dynamic dimension of the spindle. The best estimation that one can possibly make is that the rate, at which the spindle diameter is lost, is higher at high temperatures and much lower at lower temperatures, so that the experimental viscosity data presented in this study may be lower than actual values. Moreover, crystallization on the spindle surface may be occurring during the experiment, making it too complicated of a case to make reasonable quantitative estimation. Therefore, the bump in the viscosity versus temperature plot in the range of 1400–1350 °C may be a mixed result of the precipitation of the crystalline phase and shrinking of the total slag/spindle contact area.

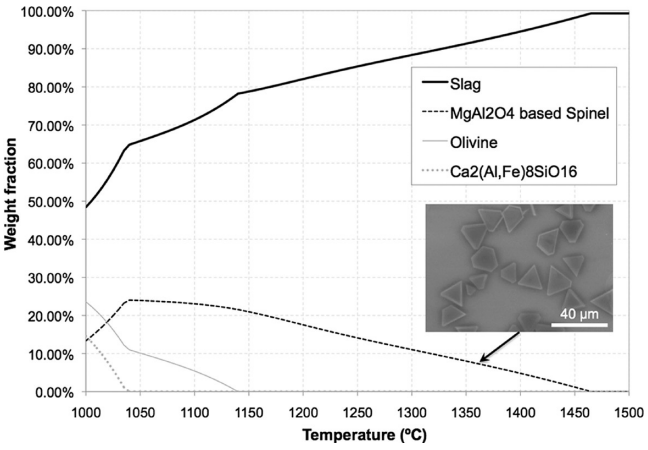

Figure 12. Crystalline phases predicted by FactSage and the SEM image of the crystals precipitated in WC.

Figure 13 shows the time–temperature–transformation (TTT) diagram of the crystallization of western coal slag made using the CSLM. Crystals precipitated very fast at all of the temperatures examined. This result showed that, when the viscosity was measured, the melt was in fact a mixture of liquid slag and crystals. Although the TTT curve seemed to have two "noses", the crystalline phase found at the two nose temperatures had no difference. The crystalline phases predicted by FactSage are given in Figure 12, which also show that the weight fraction of crystals in the melt should increase with lowering temperatures. In the temperature range of 1200–1500 °C, the only crystalline phase predicted and observed while obtaining the TTT diagram was the $MgAl_2O_4$ spinel. A SEM micrograph of the crystals is shown in Figure 12. Spinel crystals precipitated at higher temperatures were usually larger but in a smaller amount than those precipitated at lower temperatures.

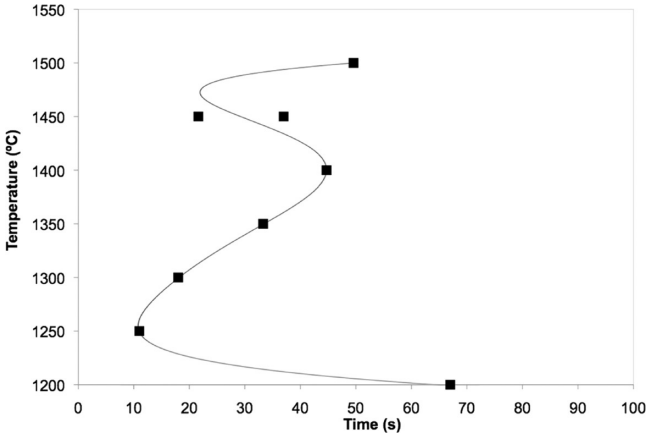

Figure 13. TTT diagram for crystal precipitation in western coal slag under $CO/CO_2 = 1.8$.

The viscosity of a slag containing both liquid and solid, $\eta_{mixture}$, can be described by the Goldsmith equation[17]

$$\eta_{mixture} = \eta_{liquid}(1 + ax + bx^2) \quad (2)$$

where x is the volume fraction of solid in the melt, η_{liquid} is the viscosity of the liquidus slag, a is a constant related to the shape of the crystal and/or crystal clusters, and b is a constant related to the solid–melt hydrodynamic interaction. Annen et al.[18] reported $a = 2.5$ and $b = 9.15$ for spherical solid at low concentrations.

As shown in Figure 12, the only type of crystal present in the slag from 1500 to 1200 °C was spinel, which had a shape that was either "equiaxed" polyhedron or truncated polyhedron, because of {111} faceting of spinel crystals.[19] Therefore, the shape of the crystals was approximated as a polyhedron. Values for constants a and b could be obtained for the western coal slag with both experimental viscosity data and model prediction values. The viscosity in data set WC-B1-M1 above 1350 °C was chosen for $\eta_{mixture}$, because the viscosity versus temperature dependence of WC-B1-M1 agreed fairly well with Kalmanovitch predictions calculated with the starting slag composition, and hence, η_{liquid} was taken as the Kalmanovitch prediction values. The weight

dx.doi.org/10.1021/ef300632x | Energy Fuels 2012, 26, 4465–4474

percentage of phases calculated by FactSage, as shown in Figure 12, was converted into volume fraction. The volume of the liquid slag was calculated using the method described by Mills et al.[20] Adopting the same form of eq 2 and fitting of the data for $\eta_{mixture}$ and η_{liquid} results in the following equation with $R^2 = 0.997$:

$$\eta_{mixture} = \eta_{liquid}(1 + 2.8858x + 10.5618x^2) + (0.1543\eta_{liquid} - 0.1118) \quad (3)$$

Because the values of the last part of eq 3 are on the order of 10^{-2}, eq 3 can be simplified into the following:

$$\eta_{mixture} = \eta_{liquid}(1 + 2.8858x + 10.5618x^2) \quad (4)$$

The values of constants a and b in eq 2 were 2.8858 and 10.5618, respectively, only slightly larger than those reported by Annen et al.[18] One should also note that the Goldsmith equation can only serve as a first approximation to describe the effect of the precipitation of the crystalline phase on the viscosity of slags because it does not take into account factors such as the size of crystallites.

In conclusion, viscosity measurements of western coal slag are challenging because such slag is corrosive to the ceramic container and spindle. Despite the dissolution of container/spindle materials into the slag, the two viscosity data sets obtained agreed best with Kalmanovitch prediction values from 1375 to 1500 °C. Precipitation of crystalline phases seems inevitable for this slag chemistry. Estimation of the constants in the Goldsmith equation with experimental viscosity data resulted in reasonable values. Nevertheless, a more corrosion-resistant container/spindle material must be used to minimize the introduction of foreign substances into the slag; also, its interaction with the slag should be minimal.

Furthermore, a possible viscosity measurement that one can experiment with is first measuring the viscosity in a cooling cycle and then reheating the slag and measuring the viscosity for a second time in a heating cycle. Differences in the viscosities during the heating and cooling cycle could be expected if crystallization have occurred, and this may offer interesting data on the impact of crystallization on the slag viscosity, especially for the western coal slag.

4. CONCLUSION

Rotating bob viscometer experiments were carried out on synthetic slags with chemistries similar to eastern and western coal slags in a low-oxygen-partial-pressure- and high-temperature-simulated gasifier environment. The following was found: (i) Iron containers and spindles used in an inert atmosphere resulted in viscosity values larger than expected as a result of metallic Fe precipitation at the slag/solid walls. (ii) The use of ceramic materials (Al_2O_3 or ZrO_2) resulted in reasonable and reproducible viscosity data for eastern coal. (iii) Viscosity measurements using ceramic parts agreed best with FactSage prediction above 1350 °C, and the Kalmanovitch prediction was best below 1350 °C, with an average activation energy of 271.2 kJ for eastern coal slag. (iv) Both the ceramic container and spindle were attacked by western coal slag, and crystallization occurred during viscometry experiments for this slag chemistry. (v) In general, viscosity data agreed best with the Kalmanovitch prediction above 1350 °C for western coal slag but deviated from the predicted viscosity values at lower temperatures likely because of precipitation of crystals in the melt. (vi) A TTT study of crystallization showed that crystallization occurred fast in the temperature range of 1200−1500 °C. (vii) An approximate relation between precipitation of the crystalline phase and slag viscosity was obtained using the Goldsmith equation.

AUTHOR INFORMATION

Corresponding Author

*E-mail: jingxiz@andrew.cmu.edu.

Notes

This report was prepared as an account of work sponsored by an agency of the United States Government. Neither the United States Government nor any agency thereof nor any of their employees makes any warranty, express or implied, or assumes any legal liability or responsibility for the accuracy, completeness, or usefulness of any information, apparatus, product, or process disclosed, or represents that its use would not infringe privately owned rights. Reference herein to any specific commercial product, process, or service by trade name, trademark, manufacturer, or otherwise does not necessarily constitute or imply its endorsement, recommendation, or favoring by the United States Government or any agency thereof. The views and opinions of authors expressed herein do not necessarily state or reflect those of the United States Government or any agency thereof.

The authors declare no competing financial interest.

ACKNOWLEDGMENTS

This technical effort was performed in support of the National Energy Technology Laboratory's ongoing research in development of coal gasification under the RES Contract DE-FE0004000.

REFERENCES

(1) Bennett, J. P.; Kwong, K.; Powell, C.; Krabbe, R.; Thomas, H.; Petty, A. *Low Chrome/Chrome Free Refractories for Slagging Gasifiers*; United States Department of Energy (U.S. DOE): Washington, D.C., 2006; Research Report DOE/NETL-IR-2006-119, pp 200−206.

(2) Browning, G. J.; Bryant, G. W.; Hurst, H. J.; Lucas, J. A.; Wall, T. F. *Energy Fuels* **2003**, *17* (3), 731−737.

(3) Selvig, W. A.; Gibson, F. H. *Bureau of Mines Bulletin 567*; United States Government Printing Office: Washington, D.C., 1956.

(4) Vorres, K. S. *Users Handbook for the Argonne Premium Coal Sample Program*; Argonne National Laboratory: Argonne, IL; http://web.anl.gov/PCS/report/part2.html.

(5) Kondratiev, A.; Jak, E. *Metall. Trans. B* **2001**, *32*, 1015−1025.

(6) Urbain, G.; Cambier, F.; Deletter, M.; Anseau, M. R. *Trans. J. Br. Ceram. Soc.* **1981**, *80*, 139−141.

(7) Bale, C. W.; Pelton, A. D.; Thompson, W. T. *Facility for the Analysis of Chemical Thermodynamics*; Ecole Ploytechnique: Montreal, Quebec, Canada, 2000; http://www.factsage.com.

(8) Kalmanovitch, D. P.; Frank, M. *Engineering Foundation Conference on Mineral Matter and Ash Deposition from Coal*; United Engineering Trustees, Inc.: Santa Barbara, CA, 1988.

(9) Vargas, S. Straw and coal ash rheology. Ph.D. Thesis, Technical University of Denmark, Lyngby, Denmark, 2001.

(10) Nakano, J.; Sridhar, S.; Moss, T.; Bennett, J. P.; Kwong, K.-S. *Energy Fuels* **2009**, *23*, 4723−4733.

(11) Orrling, C.; Sridhar, S.; Cramb, A. W. *High Temp. Mater. Processes* **2001**, *20* (3−4), 195−199.

(12) Orrling, C.; Sridhar, S.; Cramb, A. W. *ISIJ Int.* **2000**, *40*, 877−885.

(13) Sridhar, S.; Cramb, A. W. *Metall. Mater. Trans. B* **2000**, *31B* (2), 406−411.

(14) Soll-Morris, H.; Sawyer, C.; Zhang, Z. T.; Shannon, G. N.; Nakano, J.; Sridhar, S. *Fuel* **2008**, *88*, 670−682.

(15) Kaneko, T. K.; Bennett, J. P.; Sridhar, S. *J. Am. Ceram. Soc.* **2011**, *94* (12), 1−9.

(16) Hrma, P.; Arrigoni, B. M.; Schweiger., M. J. *J. Non-Cryst. Solids* **2009**, *355*, 891−902.
(17) Goldsmith, H. L.; Mason, S. G. *Rheology, Theory and Application*; Academic Press: New York, 1967.
(18) Annen, K.; Gruninger, J.; Stewart, G. *Proc. Flames Res. Found.* **1983**, 1−3.
(19) Carter, C. B.; Rasmussen, Y. K. *Acta Metall. Mater.* **1994**, *42* (8), 2729−2740.
(20) Mills, K. C.; Keene, B. J. *Int. Mater. Rev.* **1987**, *32*, 1−120.